International Journal of Minerals, Metallurgy and Materials
Accepted manuscript, https://doi.org/10.1007/s12613-020-2032-1

Non-spherical Aluminum nanoparticles fabricated using picosecond laser ablation

A. Brahma Swamulu[1,3], *S. Venugopal Rao*[2], *and G Krishna Podagatlapalli*[1]

1) Department of Electronics & Physics**,** GITAM Institute of Science, GITAM deemed to be University, Visakhapatnam 530045, Andhra Pradesh, India.

2) Advanced Centre of Research in High Energy Materials **(ACRHEM),** University of Hyderabad, Hyderabad 500046, Andhra Pradesh, India

3) Department of Physics**,** Rajiv Gandhi University of Knowledge Technologies, Nuzvid, Andhra Pradesh-521202, India

Corresponding author: G Krishna Podagatlapalli Email: **gopalakrishna.podagatlapalli@gitam.edu**

Abstract

In this article, we report the picosecond laser ablation of Aluminum targets immersed in a polar organic liquid [chloroform ($CHCl_3$)] with ~2 ps laser pulses at an input energy of ~350 μJ. The synthesized Aluminum nanoparticles exhibited a surface plasmon resonance peak at ~340 nm. Scanning electron microscopic images of Al NPs demonstrated the spherical morphology with an average size ~27±3.6 nm. The formation of spherical Al nanoparticles at smaller dimension and seizing of further growth could be from the formation of electric double layers on the Al nanoparticles. In addition to spherical Aluminum nanoparticles, triangular/pentagonal/hexagonal nanoparticles were also observed in colloidal solution. Field Emission Scanning Electron Microscopic images of ablated Al targets demonstrate laser induced periodic surface structures (LIPSS). These are the high spatial frequency LIPSS (HSFL) since their grating period was ~270 nm. Additionally, coarse structures with a period ~700 nm were also observed.
Keywords: Ablation, Picosecond, Silver, polar, periodic surfaces, Electric double layers

1. Introduction

In the last few decades, many physical and chemical methods were introduced to synthesize nanoparticles and nanostructures such as ball milling, sputtering, sol-gel method, physical vapour deposition, laser ablation etc. Amongst laser ablation of metal targets in which an intense laser light irradiates a metal target results in the formation of nanoparticles [1-9]. When ablation is carried out in air there always be a likelihood of contamination of the medium around due to the expulsion of nanoparticles into the medium. This disadvantage can be fixed by performing the ablation by keeping the metal target (thereby restraining the plasma) in a liquid. Laser ablation of metal targets (Aluminum, Gold, Silver, Platinum etc.) immersed in liquid medium gained a lot more attention by the scientific community due to its simplicity and versatility. This technique enables the fabrication of nanoparticles and nanostructures in a single experiment which is a few minutes job. When a target immersed in a liquid irradiated by an intense laser light, due to the local heating metallic plume will be produced on the target surface. Subsequently, liquid layer adjacent to the metallic plume gets evaporated, consequently, it exerts a recoil pressure on the metallic plume that splashes into spherical particles and releases into the liquid in which ablation is taking place. Nanoparticles can be obtained in colloidal form and laser ablation is the only physical technique that produces nanoparticles and nanostructures with desired roughness in a single experiment. Unlike the existing wet chemical methods, laser ablation in liquids does not need vigorous sample preparation and the usage of surfactants.

Laser-matter interaction in laser ablation is a complicated phenomenon which takes place underneath the liquid layer. The laser-matter interaction simultaneously depends on laser parameters, liquid parameters, inherent characteristics of the metal target. One more advantage of laser ablation of metals in liquid media is the possibility of gram scale green synthesis. Laser ablation of metallic targets in a liquid medium significantly depends on the polarity of the liquid. When ablation is carried out in a polar medium [10-12], molecules of the liquid in which ablation is being done will be adsorbed on the fabricated primary nanoparticles those formed initially. The outcome of laser ablation comprises ions, molecular clusters, atom, etc. Thus produced primary nanoparticles grow by the nucleation of the ions in the cavitation bubble. This growth mechanism determines

the average sizes and shapes of the nanoparticles in the colloidal solution. During the growth process, atomic clusters come closer and will be attached to the pre-existing nanoparticles.

Aforesaid growth of nanoparticles or secondary nucleation is determined by the charge on the surface of primary nanoparticles. If the charge on the primary nanoparticles is positive or negative, growth is profound due to the attractive forces of unlike surfaces. Consequently, the average size of the nanoparticles increases. The adsorption of the molecules with a particular polarity on the surface of pre-existing nanoparticles with oppositely charged surfaces creates electric double layers (EDL) which neutralizes the nanoparticles. Consequently, further growth of nanoparticles seizes and result in the formation of nanoparticles with small average sizes [13]. Ablation of Aluminum (Al) target in chloroform which is a strong polar liquid, leads to the formation of small Al nanoparticles. Additionally, nanostructures were also observed on Aluminum target where the ablation has taken place. The interaction of vapor of the liquid with the metallic melt layer results in Rayleigh-Taylor or Kelvin-Helmholtz instabilities, consequently, results in the redistribution of molten layer forms mushroom-like or dome-like structures on the ablated surfaces [14,15]. The dynamics of ablation and its outcomes as the function of laser parameters were extensively studied by Barcikowski et al. [16].

Laser exposure on Aluminum target leads to morphological modifications such as ripples [17-22], conical structures. Aluminum metal exhibits a significant value of electron-phonon coupling coefficient (γ) that facilitates the formation of ripple/grating structures. The grating s formed on the Aluminum targets can be described as the laser induced periodic surface structures (LIPSS). LIPSS again classified as high spatial frequency LIPSS when the grating period (Λ) is less than the wavelength of light utilized for the ablation. Earlier a few researchers documented [23-26] the ablation of Al in different liquid media but there are not many works describing the effect of liquid polarity on the products of the ablation.

Laser induced periodic surfaces are very exciting elements those can be produced by laser ablation in liquids. Plasmonic nanomaterials such as silver, gold, or copper spherical nanoparticles or nanostructures are having broad applications in all the areas of science. Apart from the mentioned plasmonic nanomaterials, Aluminum nanomaterials are equally exciting due to their unique optical properties. Aluminum is an economic metal with very low melting temperature 660 ^{o} compared to any other plasmonic metal. Aluminum nanomaterials have tremendous applications in defense science. In particular, Aluminum nanomaterials can be utilized as additives in propellants, pyro techniques [27] since Al nanoparticles releases gigantic amount of heat during their exothermal oxidation. To achieve gigantic heat release from Al nanoparticles, one has to synthesize pure Aluminum nanoparticles without oxidization which is a tedious task since Al can be easily oxidized. Detonation velocity and burn rate of an explosive decreases rapidly as the Aluminum nanoparticles added to it are oxidized. To achieve the non-oxidized Al nanoparticles, we attempted the laser ablation in oxygen free organic liquids such as chloroform which significantly diminish the instant oxidation of Al nanoparticles at the time of their generation. Once after synthesizing the Al nanoparticles, colloids are preserved in air tightened bottles to prevent the further oxidation due to environmental oxygen. The main advantage of laser ablation of Al target in polar liquids such as chloroform is the formation of electrical double layers (EDL) on the surface of the primary Al nanoparticles. Thus, formed EDLs neutralizes the further growth and hence the Al nanoparticles with smaller sizes can be synthesized.

2. Experimental techniques

Laser ablation of Aluminum targets immersed in chloroform were performed using a Ti:Sapphire laser system which delivers nearly transform limited laser pulses of ~2 picoseconds (ps) [repetition rate of 1 kHz, 800 nm central wavelength]. Aluminum target was submerged in chloroform ($CHCl_3$) liquid layer (2-3 mm above the target surface). It was ensured that the Al target immersed in chloroform was exactly parallel to the surface of the optical bench. Aspherical convex lens of focal length ~8 cm was utilized to focus the laser beam on to the target surface. It is so difficult to focus the laser light beam exactly on Al target surface immersed in the chloroform due to the refractive index of the medium. Refractive index of the medium displaces the focal plane beyond the position of the focus in the absence of liquid. This displacement of the focus results in the poor rate of ablation and, consequently, lower yields of NPs. To avoid this, the focal plane of the laser beam was adjusted by displacing the target or lens. The estimated beam waist (ω_0) at the focus in air was estimated to be ~15 µm. The petri dish comprising chloroform immersed Al target was placed on a motorized X-Y stage, which can be operated through the motion controller. The utilized energy per pulse is estimated to be ~350 µJ. Two motorized linear stages (X and Y) mediate by a motion controller (Newport ESP 300) to move with speeds 0.2 mm/sec, 0.4 mm/sec, respectively. Both of the motorized stages operated in such a way to draw parallel lines on the Al sample, at a separation of ~150 µm. Time of laser irradiation was ~ 5 minutes and each scan gives 20 periodic lines on the Aluminum target. Complete details of the experimental arrangement of ultrafast laser ablation of metal targets in liquid can be seen in our earlier works [28]. While adjusting the focal plane of the lens on the surface of the target, one has to ensure the process of ablation by looking at the visible plasma generated at the point of laser irradiation. Additionally, a cracking sound made by the laser irradiation during the laser ablation is another confirmation that the focus is exactly on the surface of the target. Post ablation, laser exposed Al targets

were taken out from the liquids and preserved after a careful cleaning. Immediate to ablation, Al colloidal solutions were characterized by UV-Vis spectrometer, Energy Dispersive Spectrometer (OX-Ford Instruments) and laser exposed portions were investigated by Field Emission Scanning Electron Microscope (Ultra 55 from Carl ZEISS) instrument. UV-Vis spectra confirmed the presence of Al NPs through exhibiting LSPR peak. In this work, we carried out the fabrication of Al nanoparticles in chloroform and simultaneously we could achieve HSFLIPSS at an optimum laser energy ~350 μJ. In addition to fine ripples, we could achieve, coarse grating of period 700 nm which is near to the incident wavelength (800 nm).

3. Results and Discussion

3.1 Spherical and non-spherical Al nanoparticles

Al colloids prepared by the laser ablation of Al targets in Chloroform with ~2ps pulses are preserved in an air tightened bottle to avoid the light exposure on them. Al colloids in chloroform exhibited yellow coloration. Prior to ablation, pure chloroform did not show any coloration but the chloroform Al colloids exhibited a golden yellow coloration is a confirmation for the formation of Aluminum nanoparticles in the chloroform. As the coloration attributed to the localized surface plasmon resonances (LSPR) of Al colloids. Al colloids were characterized by UV-Vis absorption spectrometer and the localized surface plasmon peak obtained to be ~324 nm. Localized surface plasmon peak of Al colloids in different organic solvents demonstrate a very weak plasmon peak but in the case of Al NPs in Chloroform it was a broad peak whose shoulder is extended to the visible region with a plasmon bandwidth (FWHM) of ~70 nm as shown in Fig. 1.

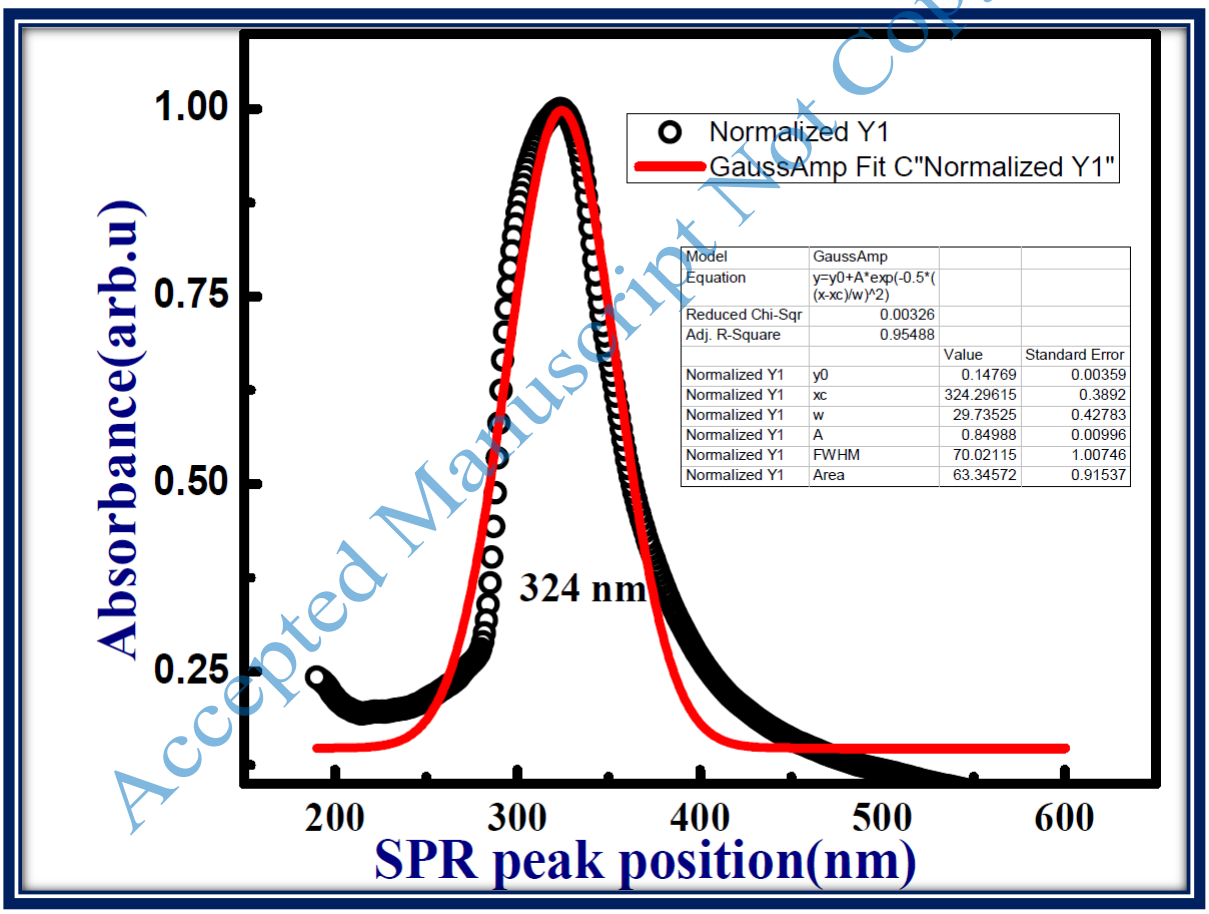

Fig. 1. UV-Visible absorption spectrum of Al nanoparticles fabricated in ~350 μJ in chloroform exhibits a LSPR peak at 324 nm.

Obtained plasmon bandwidth demonstrate the formation of Al nanoparticles with different sizes. Though the SPR peak position was in UV region, coloration of the colloidal solution is golden yellow. This is due to the extension of the shoulder of the recorded UV-Vis spectrum into the visible region. To find out the morphology of Al nanoparticle fabricated in chloroform, FESEM characterization was carried out. The FESEM data obtained from the Al colloidal solutions demonstrated that most of the synthesized Al nanoparticles were spherical in nature.

FESEM images demonstrated well mono-dispersed Aluminum nanoparticles with different sizes. FESEM image showed that Al nanoparticles with larger as well as smaller sizes are also there. As the profile of the laser beam utilized for ablation is Gaussian, the trend of ablation occurred at the center of the laser beam is not same as the ablation carried out at the shoulders of the laser beam. Consequently, the products of ablation were also different as we observed in figure 2.

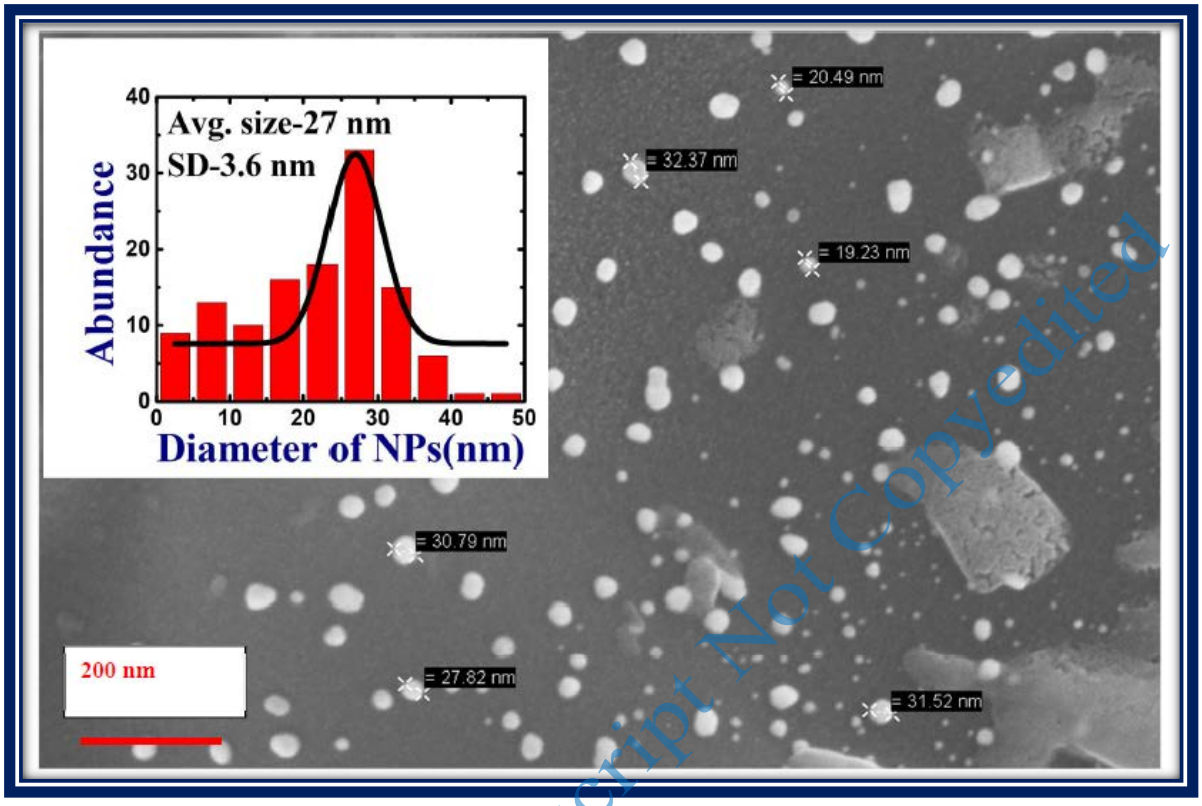

Fig. 2. FESEM image of Al nanoparticles in chloroform which demonstrate the spherical nature of Al nanoparticles. Figure in the inset shows the histogram of Al NPs whose average size was estimated to be 27±3.7 nm.

Fig. 2. depicts the FESEM image of Al NPs taken on a carbon strip. The average size of the Al nanoparticles obtained using image J software was found to be 27±3.6 nm. To estimate the average sizes four FESEM images recorded at various location on the carbon tape were considered in image J processing. Histogram was constructed by considering the estimated sizes as a whole and the estimated average size was 27±3.6 nm. In addition to the spherical nanoparticles, it was observed that triangular, pentagonal, and hexagonal. Al nanoparticles were synthesized in chloroform but their density is minimum. Fig.3. illustrates the synthesized Al nanoparticles with different morphologies. During the process of ablation, cavitation bubble is formed and the properties of cavitation bubble such as its volume, expansion velocity, and life time influence the nucleation, growth mechanism and hence the final shape of nanomaterial [29,30]. At present we could only understand the formation using above-mentioned explanation and detailed experiments are being taken up to comprehend why Al nanoparticles are synthesized with these morphologies. When a metal target immersed in a liquid medium is irradiated by focused ultrafast laser pulse, local melting takes place and metallic plume is generated on the target surface. The plume comprises atoms, molecules, ions, atomic clusters etc. The liquid layer adjacent to the plume gets evaporated and during this process it exerts a pressure on the metal plume. The surface tension forces in the metallic melt keeps on trying to maintain the spherical nature of the plume. But the recoil pressure is gigantic and hence the metallic melt splashes into particles. As this recoil pressure is balanced by surface tension forces, particles produced are predominantly spherical in nature. Other side of the reason for the morphologies are the cavitation bubble and its dynamics. Cavitation bubble (CB) is the cavity formed by the shock wave produced by the metallic plume during its expansion. The morphologies of the particles synthesized depends on the pressure

and temperature inside the cavitation bubble. The dynamics of CB also determined by the liquid parameters in which the ablation is being done. This is evident from the Raleigh-Plesset (RP) model. The formation of nanomaterials with different sizes and morphology can be described as the outcomes of oscillations, collapse of cavitation bubble as explained by Raleigh-Plesset (RP) equation [31] as shown in equation 1. The pressure inside the cavitation bubble is determine by the liquid parameters such as polarity, viscosity, etc. In laser ablation, the formed cavitation bubble comprises metal condensates along with liquid vapour. Consequently, these complicated interactions demonstrate the morphologies of the synthesized nanoparticles. The RP equation is given in equation number 1 as

$$R\frac{d^2R}{dt^2}+\frac{3}{2}\left(\frac{dR}{dt}\right)^2=\frac{1}{\rho}\left(\left(p_0-p_v+\frac{2\sigma}{R_0}\right)\left(\frac{R_0}{R}\right)^{3\gamma}-p_0+p_v-\frac{2\sigma}{R_0}-\frac{4\eta}{R}\frac{dR}{dt}\right) \quad \textbf{[1]}$$

The solution of the above equation describes the complete characteristics of synthesized nanomaterials on the basis of cavitation bubble dynamics.

Along with spherical Al NPs, there were nano Al triangles, pentagons and even hexagons [see the image presented in figure 3] in the colloidal solution. But their density was observed to be less and, hence, they could not modify/influence the UV-Visible absorption peak [Fig. 1.] significantly.

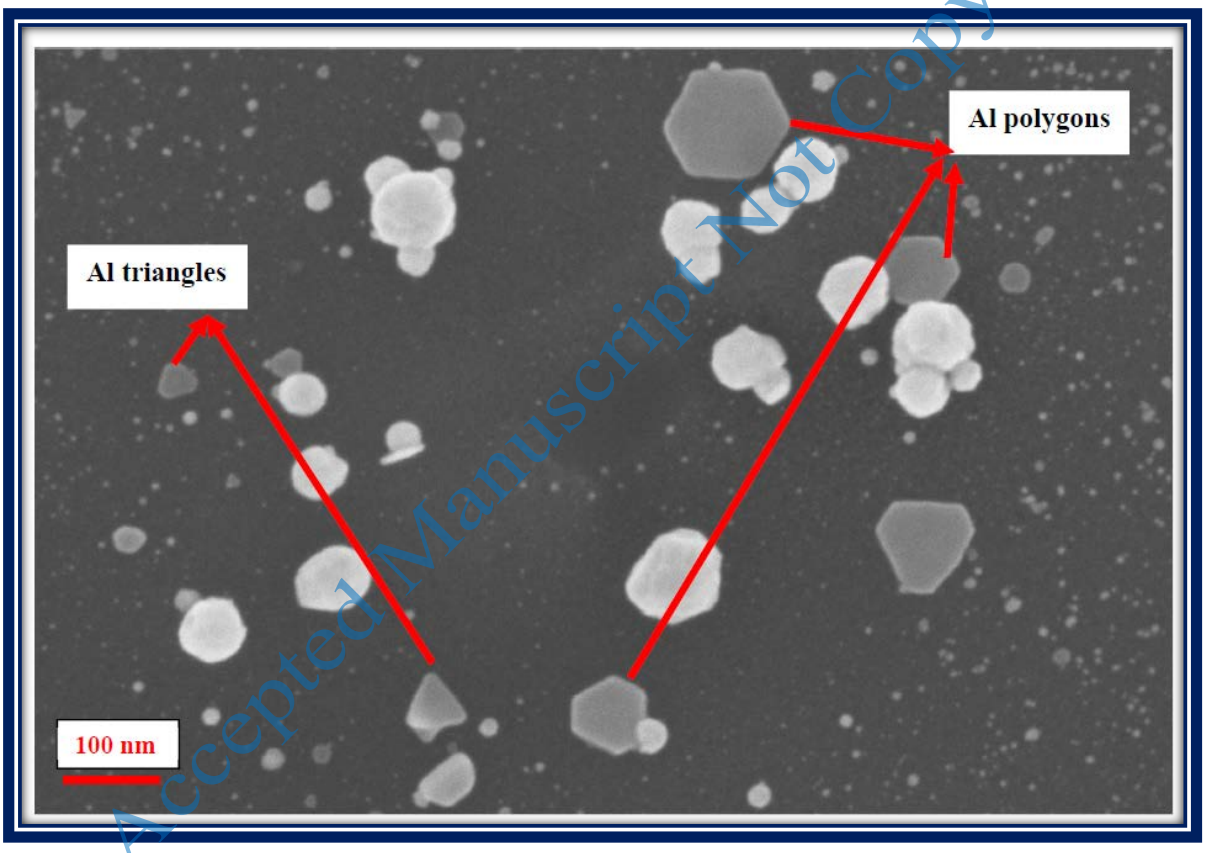

Fig. 3. FESEM image of Al nanoparticles in chloroform which demonstrate the non-spherical nature of Al nanoparticles. Pentagonal and triangular Al nanoparticles can be observed in the figure.

Origin of these triangular or polygonal nanoparticles is yet to be understood. This kind of Al NPs with different shapes is active elements for tuning the LSPR peaks to near IR from UV regions and have many plasmonic applications. According to the existing literature, many researchers reported the formation of spherical nanoparticles in the ultrafast laser ablation but no one report on the formation of such triangular or hexagonal nanoparticles. Consequently, we do not have a clear picture on the theoretical base of this kind of structures. Further studies are needed to give a clear picture of non-spherical formation of nanoparticles. Though the spherical nanoparticles are predominant, we could count the number of the triangular/pentagonal/hexagonal Aluminum nanoparticles with an extreme care and was found that the ratio of spherical to other morphologies is

50: 1. Though the number density is not high, further studies are needed to evaluate the origin of the nanoparticles with morphologies other than spherical. Ablation of Aluminum targets immersed in polar organic liquid chloroform was carried out with the laser pulses of duration ~2 picoseconds. A pulse is said to be ultrashort when its pulse duration is shorter than the electronic response/relation times of materials (~1 ps). Thus, the 2 ps pulses utilized in the present experiment are more or less considered to be ultrashort pulses. Ultrafast laser ablation of metals in liquid media is a well-known in the contemporary scientific method to synthesize nanoparticles. Majority of the reports say that the nature of the synthesized nanoparticles is **spherical.** In the present study, in addition to the spherical nanoparticles, we found the traces of non-spherical nanoparticles also. As the pulse duration is short, the complicated laser mater interaction underneath the liquid medium might led to the formation of non-spherical nanoparticles.

Recently Barcikowski et al. [32] reviewed ultrafast laser ablation and the inherent mechanisms involved in the formation of nanoparticles with different morphologies. According to them laser ablation in liquids follow three stages, first-plasma stage, second-vapor (or cavitation bubble stage), third-interaction of nanoparticles with the molecules of the surrounding liquid medium after the collapse of cavitation bubble. Immediate to the laser irradiation beyond a threshold intensity (10^9 W/cm^2), plasma is generated on the target surface. During the expansion of the plasma cavitation bubble will be created. Cavitation bubble dynamics only determines the morphologies of the synthesized nanoparticles.

3.2 Laser Induced Periodic Surface Structures (LIPSS) of Aluminum

Along with the Al colloids of spherical and non-spherical morphologies, laser exposed portions of Al exhibited mushroom type structures due to Rayleigh instabilities occur due to the strong interaction of plasma plume with the surrounding liquid medium. FESEM analysis of laser exposed Al targets ablated in $CHCl_3$ demonstrated laser induced periodic surface structures (LIPSS). Fig.4. illustrate the FESEM images of ripple structures formed on the ablated Al metal target.

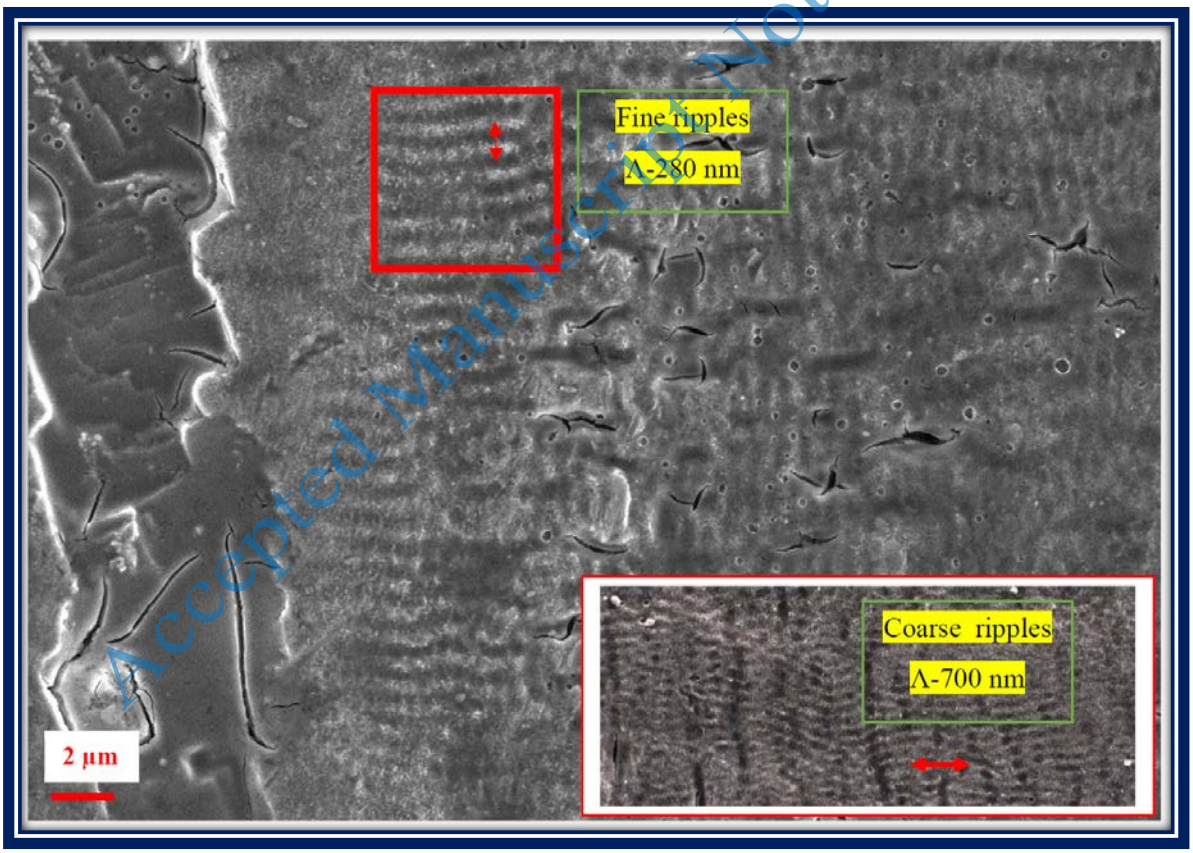

Fig. 4. Fig. 4. FESEM images of Laser induced periodic surface structures obtained on Al target surface when ablated in $CHCl_3$ with ~2 ps laser pulses [Inset shows the magnified view of Coarse ripples}.

These surface structures are the resultant of interference of the incoming electric field of the laser beam with the surface electromagnetic waves (SEW) those produced on the target surface [33]. Depending on the grating period (Λ) these surface structures are said to be high spatial frequency (HSF) LIPSS (grating period much less

than the incident wavelength) and low spatial frequency (LSF) LIPSS (grating period comparable to incident wavelength). In other words, former are called as coarse ripples and latter are the fine ripples [34]. Exact dynamics which evoke the periodicity of the surface structures is not yet understood completely. FESEM image of the laser exposed Al target demonstrated the presence of coarse ripples whose orientation was parallel to the input polarization and fine ripples which were oriented parallel to the input beam polarization. These coarse and fine ripples were not formed individually but mixed with each other. Grating period of the coarse structures was ~700 nm and grating period of fine structures was about ~280 nm as evident from the Fig. 4. Coarse grating (LSF LIPSS) was perpendicular to the polarization of the incident beam whereas fine grating was parallel to the input beam polarization. Though the formation of ripples on different materials such as semiconductors/metals/dielectrics is a longstanding puzzle, many theories are there in scientific community to explain the origin of their formation.

According to Sipe et al. [35] these ripples could be due to the interference of the incident wave and the surface scattering electromagnetic wave caused by the roughness of the sample. This interference modulates the periodic electric field on the surface results in the formation of LIPSS. Formation of gratings near the scratch indicates that the surface roughness is the primary reason for the broken symmetry and leads to the formation of grating. They described the formation of the damaged structures using electromagnetic theory, according to which, periodic damage patterns are the resultant of inhomogeneous absorption of laser energy beneath the surface. These are mediated by the intrinsic surface roughness of the metal. Soileau et al. [36] demonstrated that the non-radiative, short range fields associated with the surface defects of the materials might cause the surface scattered waves. Huang et al. [37] described the formation of the grating structure on the basis of propagating surface plasmon (PSPs) and their excitation by the incident laser pulse. Reif et al. [38] have taken a different stand on the mechanism of grating formation. They described that self-organized structures are due to the non-stable metallic plume formed in the due course of ablation. In this process the direction of the input laser electric field plays a role of driving force in the formation of self-organized surface structures under the influence of an ultrashort pulse. Other reason behind the formation of grating structure may be the complex refractive index of laser exposed portions of the target on which irradiation was carried out. Due to the impact of laser pulses effective number of charged carriers (mostly electrons) generated at the site of laser impact dramatically modify the complex refractive index of the material locally. This localized refractive index variations cause ripple structures. In addition to the complex refractive index, polarization of the incident field is another parameter which influences the orientation of the ripple pattern. Polarization of the input field influences the produced plasma and orients the ripples accordingly. Thus, the fabrication of ripples and their periodicity depend on the polarization of input beam, angles of incidence, and speed of scanning.

Coarse ripples can be observed at higher intensities [due to central portion of the laser focal spot] [39,40] and fine ripples might due to the complex refractive index of the modified surface. Period of the grating [41] is given by the equation 1,

$$\Lambda = \frac{\lambda}{1 \pm Sin\theta} \qquad [1]$$

Where θ is the angle of incidence and for normal incidence it is 0^o. Thus, for the case of metals the periodicity almost equals to the wavelength of the light utilized. Compared to silver and gold, probability of ripple formation on Aluminum targets is pretty large due to its large electron-phonon coupling constants. Experimental verification of the mentioned concept is under progress.

Metallic LIPSS support the excitation of propagating surface plasmons (PSP) wherein the grating period plays a crucial role in momentum conservation of the incident photon as mentioned in the following equation,

$$K_{parallel}(photon) = K_{parallel}(surfaceplasmawave) + n\frac{2\pi}{\Lambda} \qquad [2]$$

When a photon incident on a metallic surface, propagating surface plasmons will be generated whose wavevector is represented by K (surface plasmon). When the parallel momentum component of an incident photon equals to the parallel momentum component of surface plasmon, then the incident light will be coupled more to the metallic surface. This is possible only when a metal surface is patterned to get an appropriate grating period (Λ) in order to provide the mismatch momentum to the surface plasmon wave. When this condition is fulfilled, incident energy can be coupled to great extent to the target surface. LIPSS has many such applications by which light energy can be couple to design solar cells, waveguides, drug delivery systems etc.

4. Conclusions

In summary, Aluminum targets were ablated using ~2 ps laser pulses at an energy of ~350 μJ in chloroform and we could synthesize spherical aluminum nanoparticles at an average size ~27 nm as well as triangular, pentagonal, hexagonal Aluminum nanomaterials. The origin of the formation triangular/pentagonal Al nanomaterials is still unclear. At the moment authors could believe the dynamics of cavitation bubble play a crucial role in the determination of the size, morphologies of ablation products. Along with the mentioned Al colloids, Al nanostructures were also formed on the laser exposed portions on the targets. Both fine and coarse ripples whose separation s were ~280 nm, and 700 nms. were obtained respectively. Former ones are known as high spatial frequency laser induced periodic surface structures (HSFL) and the latter one is known as low spatial frequency laser induced periodic surface structures (LSFL). It was observed that the polarity of the chloroform molecules seizes the further growth of Al nanoparticles by the formation of electrical double layers (EDL).

5. Acknowledgements

Authors acknowledge Advanced Centre of Research in High Energy Materials (ACRHEM) labs, University of Hyderabad, India.

References

[1]. S. I. Dolgaev, A. A. Lyalin, A. V. Simakin, V. V. Voronov, and G. A. Shafeev, Fast etching and metallization of via-holes in sapphire with the help of radiation by a copper vapor laser, Appl. Surf. Sci., **109/110** (1997), p.201.

[2]. A. V. Simakin, V. V. Voronov, N. A. Kirichenko and G. A. Shafeev, Nanoparticles produced by laser ablation of solids in liquid environment, Appl. Phys. A, **79** (2004), No. 4-6, p.1127.

[3]. P. V. Kazakevich, A. V. Simakin and G. A. Shafeev, Formation of periodic structures upon laser ablation of metal targets in liquids, Quantum. Electron. **35** (2005), No. 9, p.831.

[4]. P. V. Kazakevich, A. V. Simakin, V. V. Voronov and G. A. Shafeev, Laser induced synthesis of nanoparticles in liquids, Appl. Surf. Sci. **252** (2006), No. 13, p. 4373.

[5]. T. S. Lau, G. Levi, F. Bozon-Verduraz, A. V. Petrovskaya, A. V. Simakin and G. A. Shafeev, Generation of nanospikes via laser ablation of metals in liquid environment and their activity in surface-enhanced Raman scattering of organic molecules, App. Surf. Sci. **254 (**2007), p.1236.

[6]. N. Barsch, J. Jacobi, S. Weiler and Barcikowski, Pure colloidal metal and ceramic nanoparticles from high-power picosecond laser ablation in water and acetone, Nanotechnology **20** (2009), No. 44, p.445603.

[7]. E. Messina, E. Cavallaro, A. Cacciola, R. Saija, F. Borghese, P. Denti, , B. Fazio, C. D'Andrea, P. G. Gucciardi, M. A. Lati, M. Meneghetti, G. Compagnini, V. Amendola and M. Marago, Manipulation and Raman Spectroscopy with Optically Trapped Metal Nanoparticles Obtained by Pulsed Laser Ablation in Liquids, J. Phys. Chem. *C* **115** (2011), No. 12, p.5115.

[8]. G. Krishna Podagatlapalli, S. Hamad, S. Sreedhar, S. P. Tewari and S. Venugopal Rao, Fabrication and characterization of aluminum nanostructures and nanoparticles obtained using femtosecond ablation technique, Chem. Phys. Lett. **530** (2012), p.93.

[9]. G. Krishna Podagatlapalli, S. Hamad, S. P. Tewari, S. Sreedhar, and S. Venugopal Rao, Silver nano-entities through ultrafast double ablation in aqueous media for surface enhanced Raman scattering and photonics applications, J. Appl. Phys. **113** (2013), No.7, p.073106.

[10]. T. E. Itiana, On Nanoparticle Formation by Laser Ablation in Liquids, J. Phys. Chem. C **115 (**2011), No. 12, p.5044.

[11]. N.G. Semaltioanos, nanoparticles by laser ablation, Crit. Rev. Sol. St. Mat. Sci., **35** (2010), No.2, p.105.

[12]. S. Venugopal Rao, G. Krishna Podagatlapalli, S. Hamad, Ultrafast laser ablation in liquids for nanomaterials and applications, J. Nanosci. Nanotech. **14** (2014), No.2, p.1364.

[13]. R.M. Tilaki, A. Irajizad, S.M. Mahdavi, stability, size and optical properties of silver nanoparticles by laser ablation in different carrier media, Appl. Phys A **84** (2006), No. 1-2, p.215.

[14]. L. D. Landau, E. M. Lifshitz,. Course of Theoretical Physics, Vol. 6: *Fluid Mechanics* (Nauka, Moscow, 1986; Pergamon, New York, 1989*)*

[15]. K. Bhupesh, Y. Dheerendra and K. T. Raj, Growth dynamics of nanoparticles in laser produced plasma in liquid ambient, J. Appl. Phys. **110** (2011), No.7, p.074903.

[16]. S. Barcikowski, A. Menendez-Manjon, B. N. Chichkov, M. Brikas and G. Raclukaitis, Generation of nanoparticle colloids by picosecond and femtosecond laser ablations in liquid flow, Appl. Phys. Lett. **91** (2007), No.8, p.083113.
[17]. E. Rebollar, J.R.V. de Aldana, I. Martı´n-Fabiani, M. Herna´ndez, D.R. Rueda,T. A. Ezquerra, C. Domingo, P.Moreno and M. Castillejoa, Assessment of femtosecond laser induced periodic surface structures on polymer films, Phys. Chem. Chem. Phys., **15** (2013), No. 27, p.11287.
[18]. J. Reif, O. Varlamova, M. Ratzke, M. Schade, H. Leipner and T. Arguirov, The role of asymmetric excitation in self-organized nanostructure formation upon femtosecond laser ablation, Appl. Phys. A: Mater. Sci. Process., **101** (2010), p.361.
[19]. J. Bonse and J. Kruger, On the role of surface plasmon polaritons in the formation of laser-induced periodic surface structures upon irradiation of silicon by femtosecond-laser pulses, J. Appl. Phys., **108** (2010), No.10, p.034903.
[20]. X. Jia, T. Q. Jia, N. N. Peng, D. H. Feng, S. A. Zhang, and Z. R. Sun, Dynamics of femtosecond laser-induced periodic surface structures on silicon by high spatial and temporal resolution imaging, J. Appl. Phys. **115** (2014), No.14, p.143102.
[21]. F. Costache, M. Henyk and J. Reif, Modification of dielectric surfaces with ultra-short laser pulses, Appl. Surf. Sci., 186 (2002), No.1, p.352.
[22]. A. Y. Vorobyev and C. Guo, Effects of nanostructure-covered femtosecond laser-induced periodic surface structures on optical absorptance of metals, Appl. Phys. A: Mater. Sci. Process., **86** (2007), No.3, p.321.
[23]. H. R. Dehghanpou, Laser wavelength and dose effects on Al nanoparticles structural formation in deionized water, J. Las. App. 28 (2016), No. 4, p.042007.
[24]. E. Stratakis, V. Zorba, M. Barberoglou, C. Fotakis and G. A. Shafeev, Femtosecond laser writing of nanostructures on bulk Al via its ablation in air and liquids, Appl. Surf. Sci. **255** (2009), No. 10, p.5346.
[25]. E. Stratakis, M. Barberoglou, C. Fotakis, G. Viau, C Garcia, and G. A. Shafeev, Generation of Al nanoparticles via ablation of bulk Al in liquids with short laser pulses, Opt. Exp. **17** (2009), No. 15, p.12650.
[26]. E. Stratakis, V. Zorba, M. Barberoglou, C. Fotakis and G. A. Shafeev, Laser writing of nanostructures on bulk Al via its ablation in liquids, Nanotechnology **20** (2009), No. 10, p.105303.
[27]. J. Suna, S.L. Simon, Thermochima Acta, The melting behavior of aluminum nanoparticles, **463** (2007), No. 1-2, p.32.
[28]. G. Krishna Podagatlapalli, S. Hamad, and S. Venugopal Rao, Ultrafast laser ablation of silver in aqueous media using Bessel beam for nanomaterials/nanostructures fabrication and applications in SERS, Las. Phys. Lett. **12** (2015), No.3, p.036003.
[29]. S. A. De Bonis, A. D. Giacomo, M. Dell'Aglio, A. Laurita, G.S. Senesi, R. Gaudiuso, S. Orlando, R. Teghil, G.P. Parisi, Carbon-Based Nanostructures Obtained in Water by Ultrashort Laser Pulses, J. Phys. Chem. C **115** (2011), No. 12, p.5160.
[30]. A. Menendez-Manjon, B. N. Chichkov, S. Barcikowski, Influence of Water Temperature on the Hydrodynamic Diameter of Gold Nanoparticles from Laser Ablation, J. Phys. Chem. C **114** (2010), No. 6, p.2499.
[31]. C. Langhammer, Z. Yuan, I. Zoric, B. Kasemo, Plasmonic Properties of Supported Pt and Pd Nanostructures, Nano Lett. **6** (2006), No. 4, p.833.
[32]. D. Zhang, B. Gokce, S. Barcikowski, Laser Synthesis and Processing of Colloids: Fundamentals and Applications, Chem. Rev. 117 (2017), no. 5, p. 3990.
[33]. P.M. Fauchet, A.E. Siegman, Surface ripples on silicon and gallium arsenide under picosecond laser illumination, Appl. Phys. Lett.**40** (1982), No.9, p.824.
[34]. D. Jost, W. Lüthy, and H. P. Weber, Laser pulse width dependent surface ripples on silicon, Appl. Phys. Lett. **49** (1986), No.11, p.625.
[35]. J.E. Sipe, J.F. Young, J.S. Preston, H.M. van Driel, Laser-induced periodic surface structure. I. Theory. Phys. Rev. B **27** (1983), No. 2, p.1141.
[36]. P. A. Temple, M. J. Soileau, Polarization charge model for laser induced ripple patterns in dielectric materials, IEEE J. Quant. Elec., **QE-17** (1981), No. 10, p. 2067.
[37]. M. Huang, F.L. Zhao, Y. Cheng, N.S., Xu, Z.Z. Xu, Origin of Laser-Induced Near-Subwavelength Ripples: Interference between Surface Plasmons and Incident Laser. ACS Nano **3** (2009), No. 12, p. 4062.
[38]. J.Reif, O.Varlamova, F. Costache, Femtosecond laser induced nanostructure formation: Self-organization control parameters. Appl. Phys. A **92** (2008), No.4, p.1019.
[39]. T. Tomita, K. Kinoshita, S. Matsuo, S. Hashimoto, Effect of surface roughening on femtosecond laser-induced ripple structures, Appl. Phys. Lett. **90** (2007), No.15, p.153115.

[40]. D. Dufft, A. Rosenfeld, S. K. Das, R. Grunwald, J. Bonse, Femtosecond laser-induced periodic surface structures revisited: A comparative study on ZnO, J. Appl. Phys. **105** (2009), No.3, p.034908.
[41]. L. Xue, J.Yang,Y. Yang, Y. Wang, X. Zhu, Creation of periodic subwavelength ripples on tungsten surface by ultra-short laser pulses, Appl. Phys. A **109** (2012), No.2, p.357.